15th Triennial World Congress, Barcelona, Spain

ESTIMATION OF PROCESS VARIABLES IN A GLASS MELTING FURNACE

Leo Huisman

Department of Chemical Engineering, Eindhoven University of Technology, 5600 MB Eindhoven, l.huisman@tue.nl

Abstract: In this paper the application of observers for glass melting furnaces is discussed. In glass melting furnaces only few variables, of those that are important for the glass quality, can be measured. Here it is demonstrated how low complexity mathematical furnace models can be used to estimate the other variables that cannot be measured.

Keywords: Luenberger observer, Kalman filter, glass melting furnace

1. INTRODUCTION

In glass melting furnaces glass is molten at high temperatures and the result is a glass melt that contains a high amount of very small bubbles (containing mainly CO_2 and N_2) and also some solid material (mainly SiO_2) that has to be dissolved in the melt. Furthermore, the glass melt may not yet be homogeneous just after melting. A sketch of a glass melting furnace is shown in figure 1. For the melting of the remaining solid particles it is important that the particles have a sufficiently long residence time in the furnace and sufficiently high temperatures along their trajectories. The small bubbles are released from the melt by letting

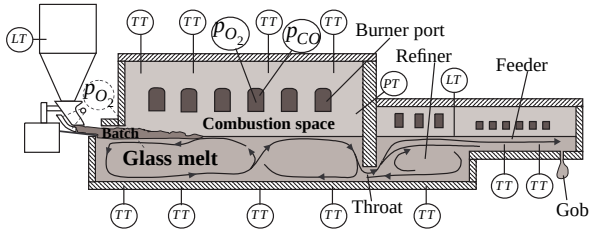

Fig. 1. Sketch of a glass melting furnace with its measurements. *TT* is temperature transmitter, *PT* is pressure transmitter, *LT* is level transmitter p_{O_2} is partial oxygen pressure and p_{CO} is partial carbon monoxide pressure. The sensor with dotted lines is a sensor for oxygen partial vapor pressure in the melt and is in a test phase.

them grow and rise to the surface. This process is called the fining process. The bubble growth is induced by a so called fining agent, that dissociates at a higher temperature than the melting temperature of the glass to form a fining gas. For the melting, fining and homogenizing processes not only the temperature is important but also the velocities in the melt. In figure 1 it is shown that temperatures in the glass melt are not measured. To determine the temperatures in important glass melt zones but cannot be reached through online measurements we use an estimator which is designed based on mathematical models that are available for the glass melting furnaces. Here the design of such estimator for glass melting furnaces is discussed. First the derivation of a relatively simple simulation model is presented. This model is used in the Kalman observer that will be discussed next.

2. MODELS FOR THE GLASS MELTING FURNACE

Glass melting tanks are often modeled with CFD-codes (computational fluid dynamics (Patankar, 1980), (Post, 1988), (Ungan and Viskanta, 1987), (Viskanta, 1994)) for design purposes or process operation improvement. Typical properties of these models are the high level of detail and high computational effort needed to do calculate a solution. If a model is used in a controller, it must allow fast enough calculations and predict the dynamic behavior in the important frequency region well enough. Fast enough would typically mean a hundred times real time and well enough

would mean that the controller will make the process meet any performance criteria one might have. Knowing this, one can verify that a CFD-code with a high number of grid points will in general be to complex. Much effort is being put in developing reduced models that are derived from a glass tank model (GTM), a CFD-code written especially for glass melting furnaces by the research institute TNO. Until these models become available testing of controllers can be done on simple test models derived from first principles or identified by using input-output data from the GTM or a real furnace. Identification of input-output data ((Haber *et al.*, 1981), (Ljung, 1987), (Wertz and Demeuse, 1987), (Wertz *et al.*, 1992)) will lead to better models for a particular furnace in a certain operating range but it can only be applied in that range and for that furnace. Here a simple model is proposed that may be useful for:

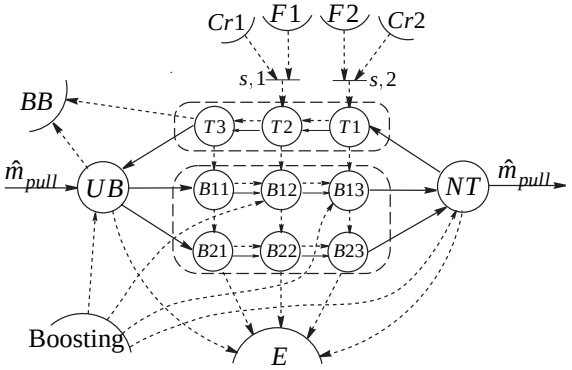

Fig. 2. Physical topology of a glass tank with a single recirculation loop.

- Gaining insight in the dynamics of the chemical and physical processes involved in the melting of glass and their effects on the overall time dependent behavior of glass melting furnaces.
- Having a flexible model available that can easily be extended or simplified and used for the design and testing of state observer or controllers and very fast simulations.

The model derived here is based on a container glass furnace for making green bottles. This furnace has in the glass melt a single recirculation loop and some smaller loops.

Table 1 : Indices used in the model description

UB	Under batch	BB	Batch blanket
B	Bottom	FS	Fuel supply
NT	Near throat	CS	Combustion space
T	Top	E	Environment

In figure 2 a physical topology is given of the glass melt, and the combustion space. It consists of systems (capacities) and connections. A circle indicates a lumped system, that is a region with uniform properties, a rounded rectangle indicates a distributed system, that is described by a partial differential equation, and an arc indicates a reservoir, a region with properties that are not influenced by in or outflows. Connections are mass flows (indicated by a solid line) or energy flows (indicated by dotted lines), that could be work or heat flows. Table 1 gives the indices of the systems in figure 1. In the next section a derivation of the model is given.

2.1 *Ideally stirred regions*

For the ideally stirred region under the batch blanket an energy equation for a constant pressure zone leads to:

$$\begin{aligned}\rho c_p V_{UB}\frac{dT_{UB}}{dt} &= \rho c_p \hat{V}_{T3|UB}\left(T_{T3}-T_{UB}\right)\\ &\quad-\alpha_{eff}A_{UB|BB1}\left(T_{UB}-T_{BB1}\right)\\ &\quad-\frac{\lambda_{wall}A_{UB|E}}{\delta_{wall}}\left(T_{UB}-T_E\right)+S_{e,UB}\end{aligned}$$

This equation can briefly be written as:

$$\begin{aligned}\dot{T}_{UB} &= f^C_{UB}\left(T_{UB},T_{T3}\right)\\ &\quad+f^D_{UB}\left(T_{UB},T_{BB1},T_E\right)+\frac{S_{e,UB}}{\rho c_p V_{UB}}\end{aligned}\quad(1)$$

Chemical reactions are assumed to take place outside region (that is in the batch blanket) and the glass is treated as a single component having average properties that depend on the composition.

The region near the throat can be modeled similarly with:

$$\begin{aligned}\rho c_p V_{NT}\frac{dT_{NT}}{dt} &= \rho c_p \hat{V}_{B13|NT}\left(T_{B13}-T_{NT}\right)\\ &\quad+\rho c_p \hat{V}_{B23|NT}\left(T_{B23}-T_{NT}\right)\\ &\quad-\frac{\lambda_{wall}A_{NT|E}}{\delta_{wall}}\left(T_{NT}-T_E\right)\\ &\quad-\alpha_{eff,NT}A_{CS|NT}\left(T_{NT,S}-T_{NT}\right)+S_{e,NT}\end{aligned}$$

This can be written as:

$$\begin{aligned}\dot{T}_{NT} &= f^C_{NT}\left(T_{NT},T_{B13},T_{B23}\right)\\ &\quad+f^D_{NT}\left(T_{NT},T_{NT,S},T_E\right)+\frac{S_{e,NT}}{\rho c_p V_{NT}}\end{aligned}\quad(2)$$

2.2 *Heat transfer in laminar flow regions*

For the laminar flow regions in the tank we can use a two dimensional model, with convective transport in the ξ_1-direction and conductive transport in the ξ_2-direction. This results in a two dimensional form of the energy equation:

$$\frac{\partial(c_pT)}{\partial t}=\frac{1}{\rho}\frac{\partial}{\partial\xi_2}\left(k_{eff}\frac{\partial T}{\partial\xi_2}\right)-v_1\frac{\partial(c_pT)}{\partial\xi_1}+\frac{S_e}{\rho}+\sum_{\forall k}\frac{\hat{q}_{wall,k}}{\rho}$$

which can be discretized (Patankar, 1980):

$$\begin{aligned}\frac{dT_{ij}}{dt} &= \frac{k_{eff}}{\rho c_p\Delta\xi_2^2}(T_{i,j+1}-T_{i,j})-\frac{k_{eff}}{\rho c_p\Delta\xi_2^2}(T_{i,j}-T_{i,j-1})\\ &\quad-\frac{\langle\bar{v}_1\rangle}{\Delta\xi_1}(T_{i+1,j}-T_{i-1,j})+\frac{S_{e,ij}}{\rho c_p}+\sum_{\forall k}\frac{\hat{q}_{wall,k}}{\rho c_p V_{ij}}\end{aligned}$$

Here, a central difference interpolation scheme for the diffusive terms and an upwind scheme for the convective terms are applied. For the top and the bottom region the following equations can be found:

$$\dot{\underline{T}}_B = \underline{f}_B^D\left(\underline{T}_B, \underline{T}_T, T_E\right) + \underline{f}_B^C\left(\underline{T}_B, T_{UB}\right) + \frac{\underline{S}_{e,B}}{\rho c_p} \quad (3)$$

$$\dot{\underline{T}}_T = \underline{f}_T^D\left(\underline{T}_T, \underline{T}_B, \underline{T}_{T,s}\right) + \underline{f}_T^C\left(\underline{T}_T, T_{NT}\right) + \frac{\underline{S}_{e,T}}{\rho c_p} \quad (4)$$

Figure 2 shows that for the bottom and top region 6 and 3 grid points (lumps) are chosen, and so $\underline{T}_B \in \mathbb{R}^6$ and $\underline{T}_T \in \mathbb{R}^3$.

2.3 *Model equations for the recirculation flow*

Multiplication of the Navier-Stokes equations with the velocity vector and integration over the entire system volume gives us an expression for the total kinetic energy change in the system (Bird *et al.*, 1960):

$$\dot{K}_{tot} = \sum_{\forall m} \alpha_m \hat{m}_m \left(\frac{1}{2}\frac{\langle \vec{v}^3 \rangle}{\langle \vec{v} \rangle} + \Phi_m + \frac{p_m}{\rho}\right) + \hat{w}_{pl} - \sum_{\forall i} E_{f,i} + \underbrace{\int_V \rho\beta v \cdot g\left(T - \bar{T}\right) d\Omega}_{\approx \sum_{\forall b} \rho\beta\langle \bar{v}_z \rangle g_z\left(\bar{T}_b - \bar{T}\right) V_b}$$

Now if one makes the assumption that the kinetic energy of the recirculating flow is only influenced by the size of the buoyancy forces in the melt, then the following form of this equation can be written:

$$\dot{K}_{rc} = -\sum_{\forall i} E_{f,i} + \sum_{\forall b} \rho\beta\langle \bar{v}_z \rangle g_z\left(\bar{T}_b - \bar{T}\right) V_b \quad (5)$$

The friction terms can be derived from the laminar flow patterns that are assumed by calculating the integral $E_{f,i} = -\int_{V_i} (\tau : \nabla v)\, d\Omega$. In this paper it is assumed that the friction losses occur in the top and bottom regions indicated by T and B in the physical topology given in figure 2 and that the flow can be modeled as one dimensional laminar flow between horizontal plates.

$$v_1 = \frac{-\gamma_i \hat{V}_i}{W H_i^3}\left(\tfrac{1}{6}\gamma_i \xi_2^2 - H\xi_2\right)$$

Two cases can be considered:

- One dimensional flow (in 1-direction) over one plate: $\gamma_i = 3$
- One dimensional flow between two plates: $\gamma_i = 6$

With these velocity profiles the accumulation term can be written as:

$$\dot{K}_{rc} = \frac{d}{dt}\int_{V_{T1}} \tfrac{1}{2}\rho\vec{v}^2 d\Omega + \frac{d}{dt}\int_{V_{T2}} \tfrac{1}{2}\rho\vec{v}^2 d\Omega + \frac{d}{dt}\int_{V_B} \tfrac{1}{2}\rho\vec{v}^2 d\Omega = \left[\frac{\left(\frac{1}{60}\gamma_{T2}^2 + \frac{1}{15}\gamma_{T1}^2\right)\frac{1}{2}\rho V_T \hat{V}_{pull}^2}{W_T^2 H_T^2} R + \frac{\gamma_B^2 \rho V_B \hat{V}_{pull}^2}{60 W_B^2 H_B^2}(R+1)\right]\frac{dR}{dt}$$

with $R = \dfrac{\hat{V}_T}{\hat{V}_{pull}}$ a dimensionless backflow ratio and γ a constant depending on the situation (one plate ore two plates). For the friction parts we can derive:

$$E_{f,T1} = \frac{3\hat{V}_T^2 \mu L_{T1}}{W_T H_T^3} \text{ and } E_{f,T2} = \frac{12\hat{V}_T^2 \mu L_{T2}}{W_T H_T^3} \quad (6)$$

$$E_{f,B} = \frac{12\hat{V}_B^2 \mu L_B}{W_B H_B^3} \quad (7)$$

and the buoyancy terms can be written:

$$\sum_{\forall b} \rho\beta\langle \bar{v}_z \rangle g_z\left(\bar{T}_b - \bar{T}\right) V_b = \left(\tfrac{1}{2} + R\right)\frac{\rho\beta g V \hat{V}_{pull}}{WL}\left(T_{NT} - T_{UB}\right)$$

Using these equations we can rewrite the equation for kinetic energy and we obtain a nonlinear differential equation for R:

$$\dot{R} = \left(f_R^B + f_R^F\right)/f_R \quad (8)$$

with

$$f_R^B = \frac{\rho\beta g V}{WL}\hat{V}_{pull}\left[\left(\tfrac{1}{2} + R\right)\left(T_{NT} - T_{UB}\right)\right]$$

$$f_R^F = 15\frac{\mu L_T}{2W_T H_T^3}\hat{V}_{pull}^2 R^2 - 12\frac{\mu L_B}{W_B H_B^3}\hat{V}_{pull}^2 (R+1)^2$$

$$f_R = \frac{\left(\frac{1}{60}\gamma_{T2}^2 + \frac{1}{15}\gamma_{T1}^2\right)\frac{1}{2}\rho V_T}{W_T^2 H_T^2}\hat{V}_{pull}^2 R + \frac{\gamma_B^2 \rho V_B}{60 W_B^2 H_B^2}\hat{V}_{pull}^2 (R+1)$$

This equation describes the acceleration of the recirculating glass, due to a change in the temperature differences in the melt. The acceleration is counteracted by the friction forces. Combination of equations (1), (2), (3), (4) and (8) gives:

$$\begin{bmatrix} \dot{T}_{UB} \\ \dot{\underline{T}}_B \\ \dot{T}_{NT} \\ \dot{\underline{T}}_{Top} \\ \dot{R} \end{bmatrix} = \begin{bmatrix} f_{UB}^C + f_{UB}^D + S_{e,UB} \\ \underline{f}_B^D + \underline{f}_B^C + \underline{S}_{e,B} \\ f_{NT}^C + f_{NT}^D + S_{e,NT} \\ \underline{f}_{Top}^D + \underline{f}_{Top}^C + \underline{S}_{e,Top} \\ \left(f_R^B + f_R^F\right)/f_R \end{bmatrix}$$

These equations can briefly be written as:

$$\dot{x}(t) = f\left(x(t), u(t), \theta\right)$$

If we define $\Delta x = x - x_{ss}$ then we can write a linear approximation near the steady state:

$$\Delta\dot{x}(t) = A\Delta x(t) + B\Delta u(t)$$

where

$$A = \left.\frac{\partial f}{\partial x}\right|_{x=x_{ss}, u=u_{ss}} \qquad B = \left.\frac{\partial f}{\partial u}\right|_{x=x_{ss}, u=u_{ss}}$$

A step response of the model that was derived here was compared with simulation results of a detailed CFD-model. Some results are shown in figure 3. Major differences occur in the steady state behavior.

3. LINEAR OBSERVERS

Suppose that in the neighborhood of a certain operating point the behavior of the glass melting furnace can be described by a linear state space model of the form:

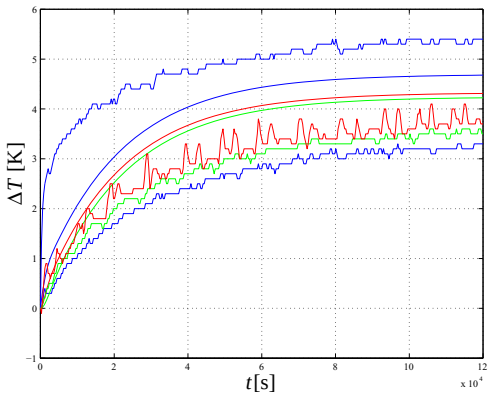

Fig. 3. Step response results of a detailed computational fluid dynamics model (CFD) and the simple simulation model (smooth curves)

$$\sigma x = Ax + Bu + w$$
$$y = Cx + v$$

where $x_{us} \in \mathbb{R}^n$ is the state vector, $w \in \mathbb{R}^n$, $v \in \mathbb{R}^p$ are disturbance vectors, $u \in \mathbb{R}^m$ is the input vector (manipulated variables), $y \in \mathbb{R}^p$ is the output vector (measured variables) and $\sigma = \frac{d}{dt}$ in continuous time and $\sigma x(t) = x(t+1)$ in discrete time. This state space model is used in an observer to estimate the state variables.

3.1 *Luenberger observer*

A type of observer that is often used is a Luenberger observer. The structure of such observer type is shown in figure 4. A Kalman filter ((Gelb, 1974), (Jazwinski,

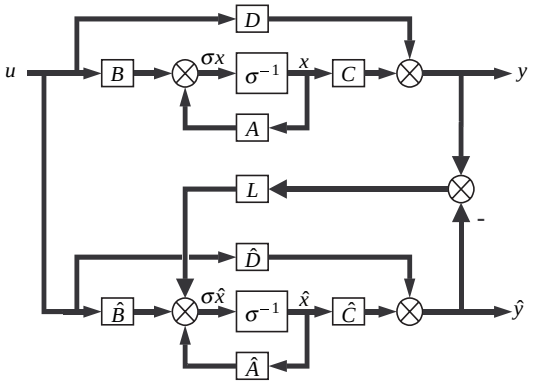

Fig. 4. Luenberger observer

1970), (Muske and Rawlings, 1993)) also has this structure and the gain matrix L is then determined such that the variance of the estimation error $\tilde{x} = x - \hat{x}$ is minimized when v and w are taken as normally distributed white noise, that is:

$$\min_{L,\hat{x}(0)} \operatorname{tr} \mathbb{E}\left(\tilde{x}(t)\,\tilde{x}(t)^T\right)$$

The solution is then found in the discrete time case through the solution of the following Discrete time Algebraic Ricatti Equation (DARE):

$$\bar{P} = A\bar{P}A^T - A\bar{P}C^T\left(C\bar{P}C^T + R_v\right)^{-1}C\bar{P}A^T + G_w Q_w G_w^T \quad (9)$$

where R_v and Q_w are the covariance matrices of the disturbance vectors v and w respectively. The solution $\bar{P}$ is the steady state value of the covariance matrix P of $\tilde{x}$:

$$\lim_{t\to\infty} P(t) = \lim_{t\to\infty} \mathbb{E}\left(\tilde{x}(t)\,\tilde{x}(t)^T\right)$$

The Kalman gain matrix L is then given by:

$$L = A\bar{P}C^T\left(C\bar{P}C^T + R_v\right)^{-1}$$

The observer equation in the discrete time case is given by:

$$\hat{x}(t|t+1) = \hat{A}\hat{x}(t|t-1) + \hat{B}u(t) + L\left(y(k) - C\hat{x}(t|t-1)\right)$$

The Luenberger configuration can be put in the standard form in figure 5 where $\tilde{P}$ can be partitioned as:

$$\tilde{P} = \begin{pmatrix} \tilde{P}_{11} & \tilde{P}_{12} \\ \tilde{P}_{21} & \tilde{P}_{22} \end{pmatrix}$$

If we take

$$\tilde{w} = \begin{pmatrix} R_v^{1/2} & 0 \\ 0 & Q_w^{1/2} \end{pmatrix}^{-1} \begin{pmatrix} v \\ w \end{pmatrix}$$

and $\tilde{w}$ as white noise with unit intensity then the Kalman filter minimizes $\left|\left|F_l(P,F)\right|\right|_2 = ||\tilde{P}_{11} + \tilde{P}_{12}(I - \tilde{P}_{22}F)^{-1}\tilde{P}_{21}||_2$. So the Kalman filter is a H_2-filter. Minimization of the 2-norm means minimizing all

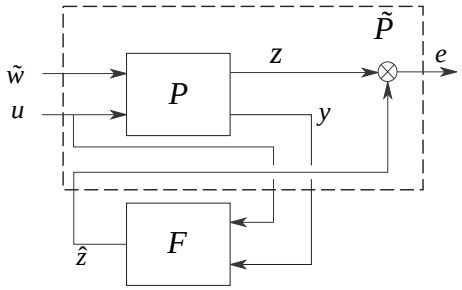

Fig. 5. Filter problem in standard form: Find a filter F such that the norm of the closed loop transfer from $\tilde{w}$ to e is minimized

singular values of the transfer matrix $F_l(P,F)$ in the entire frequency range. By filtering the white noise disturbances (coloring) emphasis can be put on important frequency ranges. Let these filters have the following state space representation:

$$\sigma x_v = A_v x_v + B_v \tilde{w}_1$$
$$v = C_v x_v + D_v \tilde{w}_1$$
$$\sigma x_w = A_w x_w + B_w \tilde{w}_2$$
$$w = C_w x_w + D_w \tilde{w}_2$$

with $x_v \in \mathbb{R}^{n_v}$ and $x_w \in \mathbb{R}^{n_w}$ Then the extended plant is described by:

$$\begin{pmatrix} \sigma x_v \\ \sigma x_w \\ \sigma x \\ y \end{pmatrix} = \left(\begin{array}{ccc|ccc} A_v & 0 & 0 & B_v & 0 & 0 \\ 0 & A_w & 0 & 0 & B_w & 0 \\ 0 & C_w & A & 0 & D_w & B \\ \hline C_v & 0 & C & D_v & 0 & D \end{array}\right) \begin{pmatrix} x_v \\ x_w \\ x \\ \tilde{w}_1 \\ \tilde{w}_2 \\ u \end{pmatrix}$$

The filter that is designed for this extended system has dimension $n_v + n_w + n$. The filter can be extended in the Luenberger setting by adopting the extended model also in the observer and then search for a gain matrix $\tilde{L} \in \mathbb{R}^{(n_v+n_w+n)\times p}$ ((Muske and Rawlings, 1993)). First we consider the case where we only have integrating coloring filters for the output disturbance v:

$$\begin{pmatrix} \sigma x_v \\ \sigma x \\ y \end{pmatrix} = \left(\begin{array}{cc|ccc} A_v & 0 & B_v & 0 & 0 \\ 0 & A & 0 & Q_w^{1/2} & B \\ \hline C_v & C & D_v & 0 & D \end{array}\right) \begin{pmatrix} x_v \\ x \\ \tilde{w}_1 \\ \tilde{w}_2 \\ u \end{pmatrix}$$

where

$$A_v = I \quad B_v = \begin{bmatrix} R_{v,1}^{1/2} & 0 \end{bmatrix}$$

$$C_v = I \quad D_v = \begin{bmatrix} 0 & R_{v,2}^{1/2} \end{bmatrix}$$

If we consider the evolution of the filter states, $\hat{x}_E$, we get:

$$\begin{bmatrix} x_v(t+1) \\ \hat{x}(t+1) \end{bmatrix} = \begin{bmatrix} I - L_1 & -L_1 C \\ -L_2 & A - L_2 C \end{bmatrix} \begin{bmatrix} x_v(t) \\ \hat{x}(t) \end{bmatrix} + \begin{bmatrix} 0 \\ B \end{bmatrix} u(t) + \begin{bmatrix} L_1 \\ L_2 \end{bmatrix} (Cx(t) + v(t))$$

Now we assume the following:

- Steady state $(t \to \infty)$, which means $\hat{x}_E(t+1) = \hat{x}_E(t)$
- $u(t) = 0$
- The system is assymptotically stable: $\lim_{t\to\infty} x(t) = 0$
- The disturbance $v(t) = \bar{v}$ remains constant (offset)

We can then write:

$$\begin{bmatrix} -L_1 & -L_1 C \\ -L_2 & A - L_2 C - I \end{bmatrix} \begin{bmatrix} x_v(t) \\ \hat{x}(t) \end{bmatrix} + \begin{bmatrix} L_1 \\ L_2 \end{bmatrix} \bar{v} = 0$$

And calculate the steady state value for the extended state $\hat{x}_E$:

$$\begin{bmatrix} x_v(t) \\ \hat{x}(t) \end{bmatrix} = - \begin{bmatrix} -L_1 & -L_1 C \\ -L_2 & A - L_2 C - I \end{bmatrix}^{-1} \begin{bmatrix} L_1 \\ L_2 \end{bmatrix} \bar{v}$$

If we use the MATLAB routine `dare` to calculate the Kalman gain matrix L and then construct $\hat{x}_E$ where the output disturbance is a constant offset $\bar{v} = \begin{pmatrix} 1 & 1 & 1 & 1 \end{pmatrix}^T$ we get for $\hat{x}_E$:

$$\hat{x}_E \approx \begin{pmatrix} \bar{x_v} \\ 0 \end{pmatrix}$$

and the error $\tilde{x}$ converges to zero. This is indeed observed and shown in figure 6. The corrections for the output offset disturbance are applied to the extra

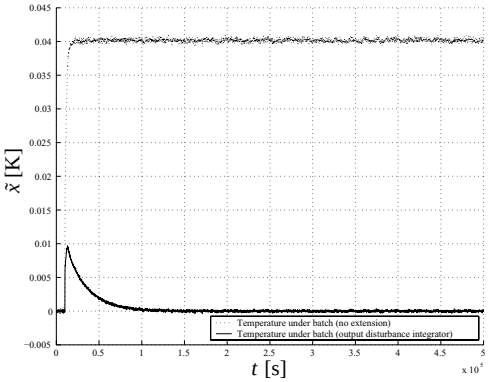

Fig. 6. The estimation error $\tilde{x} = x - \hat{x}$ of a variable that is not measured: the temperature in the region under the batch blanket (disturbance: first a step and then also a ramp).

filter states x_v that were added to the observer. If we consider the case we only have an input disturbance filter we get:

$$\begin{pmatrix} \sigma x_w \\ \sigma x \\ y \end{pmatrix} = \left(\begin{array}{cc|ccc} A_w & 0 & 0 & B_w & 0 \\ C_w & A & 0 & D_w & B \\ \hline 0 & C & R_v^{1/2} & 0 & D \end{array}\right) \begin{pmatrix} x_v \\ x \\ \tilde{w}_1 \\ \tilde{w}_2 \\ u \end{pmatrix}$$

The evolution in discrete time of the observer state $x_E(t)$ is then given by:

$$\begin{pmatrix} x_w(t+1) \\ \hat{x}(t+1) \end{pmatrix} = \begin{pmatrix} A_w & -L_1 C \\ C_w & A - L_2 C \end{pmatrix} \begin{pmatrix} x_w(t) \\ \hat{x}(t) \end{pmatrix} + \begin{pmatrix} 0 \\ B \end{pmatrix} u(t) + LCx(t) + LR_v^{1/2} \tilde{w}_1(t)$$

Now if we make again some assumptions:

- We only have a constant offset on the state variables: $\tilde{w}_2(t) = \bar{w}_2$
- $u(t) = 0$ and $\tilde{w}_1(t) = 0$
- Steady state: $x_E(t+1) = x_E(t)$

With these assumptions we get:

$$0 = \begin{pmatrix} A_w - I & -L_1 C \\ C_w & A - L_2 C - I \end{pmatrix} \begin{pmatrix} x_w(t) \\ \hat{x}(t) \end{pmatrix} + LCx(t)$$

If we choose $A_w = I$ and $C = I$ then we would expect the error $\tilde{x} = x - \hat{x}$ to converge to zero. Results are shown in figure 7 and 8. After applying a step disturbance the error converges to zero for this type of Kalman filter.

Finally, we can add both an input and an output filter. Then the states of the observer $\hat{x}_E$ satisfy:

$$\begin{pmatrix} \sigma x_v \\ \sigma x_w \\ \sigma \hat{x} \end{pmatrix} = \begin{pmatrix} A_v - L_1 C_v & 0 & -L_1 C \\ -L_2 C_v & A_w & -L_2 C \\ -L_3 C_v & C_w & A - L_3 C \end{pmatrix} \begin{pmatrix} x_v \\ x_w \\ \hat{x} \end{pmatrix} + \begin{pmatrix} 0 \\ 0 \\ B \end{pmatrix} u + \begin{pmatrix} L_1 \\ L_2 \\ L_3 \end{pmatrix} (Cx + C_v v)$$

In this case offsets lead to steady state estimation errors. Results are shown in figure 9. If both input

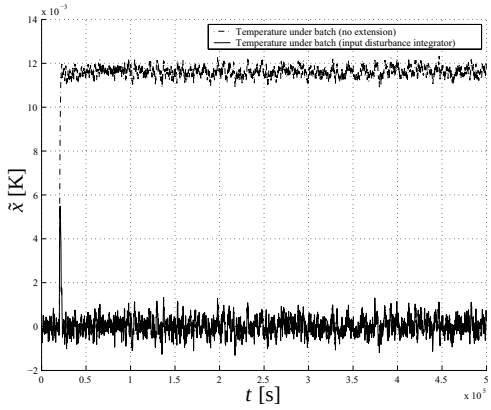

Fig. 7. Response to an input disturbance (first a step and then also a ramp). In this case $C = I$

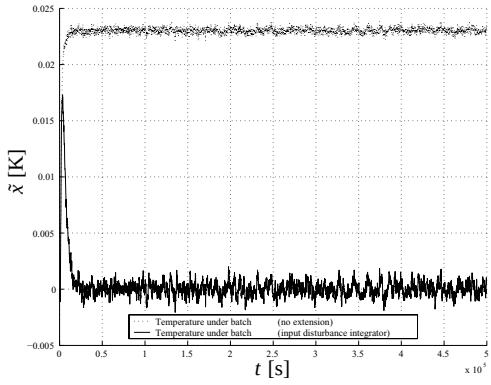

Fig. 8. Response to an input disturbance. In this case $C = [0\ I\ 0]$.

and output disturbances are present as discussed above then no improvements if compared with the ordinary Kalman filter are observed, up to now. In glass melting furnaces low frequency input disturbances (like load changes and changes in cullet properties) are most likely to occur.

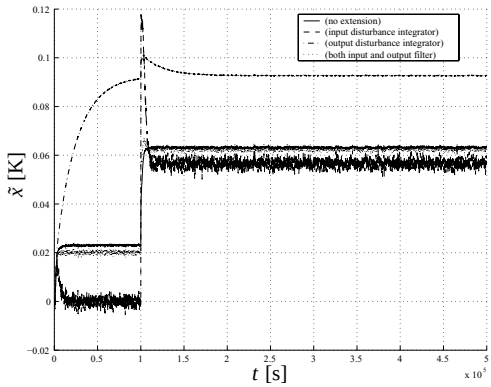

Fig. 9. Response to input and output disturbances. In this case $C = [0\ I\ 0]$.

4. CONCLUSIONS

A relatively simple simulation model was derived. Simulation results obtained with this model were compared with a detailed simulation model that takes large simulation times. The simple simulation model approximates the dynamics of the detailed model quite well. The obtained simulation model can be linearized and used in a Kalman filter to estimate state variables that are not measurable but important for the glass melting process. Effects of disturbances than white noise (e.g. offsets because of sensor aging) can be dealt with in the Kalman filter by extending the assumed process model with coloring filters.

5. REFERENCES

Bird, R.B., W.E. Stewart and E.N. Lightfoot (1960). *Transport Phenomena*. Wiley.

Gelb, Arthur (1974). *Applied optimal estimation*. The M.I.T. press.

Haber, R., J. Hetthessy, L. Keviczky, I. Vajk, A. Feher, N. Czeiner, Z. Csaszar and A. Turi (1981). Identification and adaptive control of a glass melting furnace. *Automatica* **17**(1), 175–185.

Jazwinski, Andrew H. (1970). *Stochastic processes and filtering theory*. Academic press.

Ljung, L. (1987). *System Identification: Theory for the User*. Prentice Hall.

Muske, Kenneth R. and James B. Rawlings (1993). Model predictive control with linear models. *AIChE Journal* **39**(2), 262–287.

Patankar, S.V. (1980). *Numerical Heat Transfer and Fluid Flow*. Hemisphere.

Post, Lourens (1988). Modeling of Flow and Combustion in a Glass Melting Furnace. PhD thesis. Technische Universiteit Delft.

Ungan, A. and R. Viskanta (1987). Three dimensional numerical modeling of circulation and heat transfer in a glass melting tank: Part 1. mathematical formulation. *Glastechnische Berichte* **60**(3), 71–78.

Viskanta, R. (1994). Review of three-dimensional mathematical modeling of glass melting. *J. Non-Cryst. solids* **177**, 347–367.

Wertz, V. and P. Demeuse (1987). Application of clarke-gawthrop type controllers for the bottem temperature of a glass furnace. *Automatica* **23**(2), 215–220.

Wertz, V., M. Gevers and J.F. Simon (1992). Adaptive control of the temperature of a glass furnace. *IFAC Adaptive systems in control and signal processing* pp. 311–316.